JOURNAL OF CATALYSIS **175,** 48–61 (1998)
ARTICLE NO. CA981974

Selective Catalytic Reduction of NO by NH_3 over Vanadium-Containing Zeolites

M. Wark,[1] A. Brückner,[2] T. Liese, and W. Grünert[3]

Lehrstuhl für Technische Chemie, Ruhr-Universität Bochum, D-44 780 Bochum, Germany

Received August 18, 1997; revised November 11, 1997; accepted November 13, 1997

Vanadium was introduced into zeolites, predominantly of ZSM-5 type, by isomorphous substitution (vanadium silicalites), by ion exchange with vanadyl sulphate solution (VO zeolites), and by chemical vapor deposition of $VOCl_3$ with subsequent hydrolysis and calcination ($(VO_{2.5})_x$–ZSM-5). The catalytic behavior of these materials in the selective catalytic reduction (SCR) of NO by NH_3 was investigated in a flow reactor at temperatures between 450 and 870 K. The speciation of the vanadium component was studied by a combination of spectroscopic techniques (UV–VIS, XPS, ESR, IR) prior to and after catalysis. Vanadyl-exchanged ZSM-5 exhibited high SCR activities, providing reaction rates comparable with that of a reference V_2O_5/TiO_2 catalyst though at higher temperatures. Isolated VO^{2+} ions could be identified as the active site for the SCR reaction. In particular, any significant contribution to the selective reaction of intrazeolite V(V) oxide aggregates, which may be formed from vanadyl cations at elevated temperatures, and of disruption products thereof, was ruled out. NO could be also reduced over $(VO_{2.5})_x$–ZSM-5 prepared via chemical vapor deposition of $VOCl_3$, which contained vanadium in extra- and intrazeolite oxide clusters and (if prepared from H–ZSM-5) VO^{2+} ions. With these preparations, SCR activity was found also with materials void of VO^{2+} ions and was assigned to the extra-zeolite vanadium oxide aggregates supported on the external zeolite surface. Conversely, vanadium silicalites were found to show low or no SCR activity at all, which indicates an inferior capability of isomorphously substituted vanadium to catalyze the SCR of NO by NH_3.

Key Words: **SCR of NO by ammonia; zeolites, vanadium-modified; XPS; ESR spectroscopy; UV–VIS spectroscopy.**

INTRODUCTION

In the catalytic technology of air pollution control, the selective catalytic reduction (SCR) of nitrogen oxides by NH_3 according to

$$4\,NO + 4\,NH_3 + O_2 \rightarrow 4\,N_2 + 6\,H_2O \qquad [1]$$

is the predominant commercial process for the abatement of NO_x in flue gases from stationary sources (1, 2). The V_2O_5/TiO_2 system forms the basis of most commercial catalysts for this reaction. Titania-supported vanadia exhibits high SCR activity in a temperature region between 500 and 750 K. The catalysts are, however, not stable at higher temperatures.

It is well known that the activity of the vanadium depends on its surface concentration ((3–5); (6) for V_2O_5/Al_2O_3, (7) for V_2O_5/ZrO_2), and this activity is thought to originate mostly from polymeric surface vanadates (3–5). Proposals for the catalytic reaction mechanism have been often formulated with sites including two adjacent vanadium species (8–10). The mechanism put forward by Topsøe *et al.* (10), which involves a V=O group with an adjacent acidic V−OH site, has been convincingly supported by IR-spectroscopic and thermodesorption studies (11, 12) and has formed the basis of a kinetic reaction model capable to describe the catalyst behavior in a wide range of process variables (12). On the other hand, the contribution of monomeric surface vanadate groups to the activity is subject to some disagreement. An almost linear dependence of the activity of V_2O_5/TiO_2 samples on the V content reported in early work of Inomata *et al.* (6) implies significant activity also of isolated species. Recently, Adams *et al.* (13) showed that monomeric V(V) oxo species anchored in Y zeolite catalyze the SCR reaction in absence of oxygen. The observed activities were, however, one to two orders of magnitude below those reported for V_2O_5/TiO_2 preparations in (4, 10, 12). In line with this, several groups classified the activity of monomeric surface vanadate as inferior to that of polymeric vanadate (3–5), although Went *et al.* (4) stated that the NO reduction is, indeed, catalyzed over monovanadate sites with a particular high selectivity for the desired reduction product N_2.

In the past decade, vanadium-containing zeolites have found considerable interest due to their catalytic properties

[1] Present address: Institute of Applied and Physical Chemistry, Bremen University, D-28334 Bremen, Germany.
[2] Institute of Applied Chemistry Berlin-Adlershof, Rudower Chaussée 5, D-12484 Berlin, Germany.
[3] To whom correspondence should be addressed. Fax: +49 234 7094 115. E-mail: w.gruenert@techem.ruhr-uni-bochum.de.

0021-9517/98 $25.00

in acid-catalyzed (methanol dehydration (14)) and redox reactions (hydroxylation of aromatics (15) and double-bond epoxidation with H_2O_2 (16), oxidative dehydrogenation (17), and ammoxidation (18) of propane). Zeolites have been rarely used as supports for vanadium in SCR studies (13, 19, 20), and only activity data measured in absence of oxygen are available for such materials. Due to the great variety of structures that can be stabilized in zeolitic environment, additional insight into the structure of active sites capable of catalyzing the SCR reaction may be expected from studies with vanadium-modified zeolites. After the recent development of synthesis strategies (21–23), vanadium silicalite material with predominantly isolated intraframework vanadium is available. Isolated vanadyl cations, VO^{2+}, on cationic sites may be introduced into zeolites by aqueous exchange (19, 24, 25). Small intrazeolite vanadium oxide clusters with ill-defined structure, which should, however, offer binuclear V entities to the gas phase, may be expected as by-products in the synthesis or as aggregation products of isolated sites. Such intrazeolite vanadium oxide clusters may be purposefully produced by variation of the pH during aqueous exchange (25) or by chemical vapor deposition (CVD) methods (26–28). In the latter case, it has been demonstrated that larger extrazeolite vanadium oxide clusters are deposited as well (28, 29).

In our study, we have measured the SCR activity of vanadium-containing zeolites (mainly of MFI-structure) and related it to the type of vanadium species present. Catalytic studies have been combined with catalyst characterization by various physicochemical techniques prior and subsequent to catalysis (UV–VIS, XPS, and ESR spectroscopies for the identification of V species, IR spectroscopy, and BET measurements for assessment of Brønsted activity and accessibility of V sites). While some of the data have been briefly communicated in (30), the present paper gives a full account of the investigation. It will be shown that the SCR reaction can be catalyzed at a high reaction rate by an isolated vanadium species (VO^{2+} ion).

EXPERIMENTAL

Materials

Vanadium silicalites. Vanadium silicalite samples were synthesized via different routes. VS-1/1 was obtained by a method proposed by Uguina *et al.* for titanium silicalite (22), where the heteroatom is introduced by impregnation of the silicon source (tetraethylorthosilicate, TEOS) with the heteroatom source (in our case $VOSO_4$, Fluka, purum grade). The cogel is then transformed into the silicalite material via hydrothermal synthesis (tetrapropylammonium-hydroxide, TPAOH, as templating agent, 443 K, 2 days) followed by calcination in air (823 K, 17 h). The vanadium content of VS-1/1 was 0.36 wt.%. VS-1/2 and VS-2/2 were synthesized via the route proposed by Thangaraj *et al.* (31), where the silicon source (TEOS) was impregnated with the vanadium source (VCl_3, Fluka, purum grade) in basic medium containing already the TPAOH template. Subsequently, hydrothermal crystallization and calcination were performed as above. The samples described originate from an attempt to increase the amount of isomorphously substituted vanadium to a level in excess of 1 wt.%, which resulted in overall vanadium contents of 1.2 and 1.7 wt.%, respectively. These composition data are summarized in Table 1, where the codes used to denote the various vanadium-modified zeolites are given as well.

Vanadyl-exchanged zeolites. Vanadyl ions were introduced into the zeolites (Na–ZSM-5, H–ZSM-5, Na–X, supplied by Chemiewerk Bad Koestritz, Germany) by exchange with aqueous solutions of $VOSO_4$ (0.01–0.05 M) at 343 K. Mostly, the solution pH was kept at 2.75–2.85 by adding H_2SO_4 (25). After threefold exchange ($\rightarrow$ VO–ZSM-5(3)), a V content of 0.70 wt.% was obtained ($\approx$25% exchange degree (Si/Al $\approx$13)). Onefold exchange typically resulted in a V content of $\approx$0.4 wt.% ($\rightarrow$ VO–ZSM-5(1a)). Vanadium may form oxide clusters in the sample when the solution pH exceeds 3, where the vanadyl sulphate becomes hydrolyzed. It was therefore attempted to produce a sample containing both VO^{2+} ions and vanadium oxide clusters by performing the exchange at a pH of $\approx$3 ($\rightarrow$ VO–ZSM-5(1b)). In this sample, the vanadium content became 0.62 wt.% after onefold "exchange."

Due to the low pH of the exchange solution, protons were introduced into the zeolites along with the vanadyl cations, which resulted in low residual Na contents of the VO–ZSM-5 materials (VO–ZSM-5(1a)—0.35 wt.%, VO–ZSM-5(1b)—0.82 wt.%, $\approx$15 and 35%, respectively, of the exchange capacity; VO–ZSM-5(3)—180 ppm). With some samples, it was attempted to remove these protons by re-exchange with a 0.05 M $NaNO_3$ solution (4 h at 293 K). Another VO–ZSM-5 portion was re-exchanged with a 0.5 M NH_4NO_3 solution under the same conditions in order to remove intrazeolite V(V) oxide clusters, $(VO_{2.5})_x$. The resulting sample will be denoted as VO^{2+}//ZSM-5. A sample containing only vanadium aggregates was also prepared starting from VO–ZSM-5. For this purpose, the starting material was calcined in air at 823 K for 48 h and subsequently subjected to a 2 M NaCl solution (4 h at 293 K) to remove the vanadyl cations ($\rightarrow$ $(VO_{2.5})_{x,\text{intra}}$//ZSM-5). All samples were thoroughly washed after the re-exchange treatment, dried, and stored over a saturated NH_4Cl solution.

Vanadium oxide clusters in/on ZSM-5. Vanadium oxide clusters were prepared by chemical vapor deposition of $VOCl_3$ (Fluka, >95% pure) from a nearly saturated nitrogen flow onto dehydrated H–ZSM-5 or Na–ZSM-5 (Chemiewerk Bad Koestritz, Germany, deposition at 373 or 523 K for 30 min; for more details see (28)). The deposits

TABLE 1

Catalytic Properties of Vanadium Zeolites in the SCR of NO by NH_3: Peak NO Conversions ($X_{NO,max}$) and Normalized Reaction Rates r(NO)/V at Peak Conversion

Code	Catalyst preparation/treatment	V content (wt.%)	$X_{NO,max}$	$T(X_{NO,max})$ (K)	r(NO)/V[a] (min^{-1})
EL10V1	Eurocat 1% V_2O_5/TiO_2	0.56	0.94 [0.50][b]	600	0.59 [0.61][b]
VO–ZSM-5(3)	Ion exchange (threefold), pH ≤ 2.8	0.70	0.90	650	0.45
VO–ZSM-5(1a)	Ion exchange (onefold), pH ≤ 2.8	0.37	0.64	670	0.62[c]
VO–ZSM-5(1b)	Ion exchange (onefold), pH ≈ 3	0.62	0.79	670	0.46
VO–X	Ion exchange, onefold	3.22	0.53	770	0.060
$(VO_{2.5})_x$–H–ZSM-5	Via CVD of $VOCl_3$	3.30	0.79 [0.48][b]	600	0.085 [0.10][b]
$(VO_{2.5})_x$–Na–ZSM-5	Via CVD of $VOCl_3$	0.70	0.38	670	0.19
VS-1/1	Synthesis modified from (22)	0.36	0.075	640	0.074
VS-1/2	Synthesis modified from (31)	1.20	(0.03)	—	(0.004)
VS-2/2	Synthesis modified from (31)	1.70	0	—	0
H–ZSM-5	—	—	0.46	870	—
Na–ZSM-5	—	—	0.08	650	—
[Without code]	VO–ZSM-5(1b), re-exchanged with $NaNO_3$	0.34	0.57	720	0.60
[Without code]	VO–ZSM-(1a), re-exchanged with $NaNO_3$	0.15	0.14	650	0.38
VO^{2+}//ZSM-5	VO–ZSM-5(1b), re-exchanged with NH_4NO_3	0.43	0.60	680	0.50
[Without code]	VO–ZSM-5(1b), calcined (48 h air, 823 K)	0.59	0.25	790	0.15
$(VO_{2.5})_{x,intra}$//ZSM-5	VO–ZSM-5(1a), 48 h air, 823 K + re-exchange with Na^+	0.12	<0[d]	—	—

Note. Feed gas: 1000 ppm NO, 1000 ppm NH_3, and 2% O_2 in He, at 94 liters g^{-1} h^{-1}.
[a] Rate of NO consumption related to total V (normalized reaction rate).
[b] Control experiment at 190 liters g^{-1} h^{-1}.
[c] r(NO)/V at 573 K: for 94 liters g^{-1} h^{-1}, 0.47 min^{-1} ($X_{NO} = 0.48$); for 190 liters g^{-1} h^{-1}, 0.68 min^{-1} ($X_{NO} = 0.35$).
[d] NO formation observed (in addition to N_2 and N_2O formation).

were hydrolyzed in moist hydrogen at 670 K and calcined in dry air at the same temperature. The vanadium content of these samples, which will be referred to as $(VO_{2.5})_x$–H–ZSM-5 and $(VO_{2.5})_x$–Na–ZSM-5, was 3.3 and 0.70 wt.%, respectively.

V_2O_5/TiO_2. The Eurocat sample EL10V1 (1 wt.% V_2O_5/TiO_2; for preparation and physicochemical characterization cf. (32)) was employed as a reference sample representative for titania-supported vanadium. Due to a relatively low BET surface area of the TiO_2 support (≈10 m^2/g), the V loading corresponds approximately to the theoretical monolayer capacity. The actual structure of the vanadia on the titania is still under debate (cf. (33)).

Methods

Catalysis. The SCR of NO by NH_3 was studied in a microcatalytic flow reactor at reaction temperatures between 450 and 870 K and at normal pressure. Prior to each run, the catalysts were pretreated in flowing He (50 ml/min) at 773 K for 1 h except for EL10V1, which was used without pretreatment. NO conversions and product yields (N_2, N_2O, NO_2) were measured with a feed gas containing 1000 ppm NO, 1000 ppm NH_3, and 2% O_2 in He at a space velocity of 94 liters g^{-1} h^{-1}, in some cases 190 liters g^{-1} h^{-1}. Analysis of the reaction mixtures was performed by mass spectrometry (N_2, NO, NO_2, the latter always negligible, NH_3 in feed gas analysis only) and nondispersive IR photometry (N_2O). The N_2 data were confirmed by parallel gas-chromatographic analyses. The ammonia conversion, which is accessible by mass-spectrometric analysis if water is monitored as well (signal separation on the basis of $m/e = 17$ and 18), was not measured at the present stage of the investigation, but was estimated from the nitrogen balance. When quantitative ammonia conversion could be assumed, the N balance, which then reflects deviations in the analyses of the remaining products, was typically in the range 100–110%. In this paper, NO conversions X_{NO} will be reported and compared with nitrogen yields Y_{N_2} calculated as the ratio between nitrogen production and NO feed rate.

UV–VIS spectroscopy. UV–VIS spectra were redorded in a Varian Cary 4 spectrometer with a Praying Mantis analyzer arrangement. The samples were pressed into 1–1.5 mm wafers, which can be regarded as being of infinite thickness in the terms of the Kubelka–Munk theory (34). The reflectance spectra were converted into the Kubelka–Munk function $F(R)$, which is proportional to the absorption coefficient. If the range $0.025 < F(R) < 3$ was exceeded, the samples were diluted by the parent zeolite (H–ZSM-5). In this paper, the spectra are presented after normalization to the height of the most intense absorption band at ≈200 nm.

X-ray photoelectron spectroscopy. XP spectra were recorded with a Leybold LHS 10 spectrometer (single-channel detection, Al$K\alpha$ radiation—1486.6 eV, power settings 12 kV · 23 mA, analyzer with constant pass-energy of

100 eV). The binding energy (BE) scale was referenced to C 1*s* = 284.5 eV, but the Si 2*p* level was used as a secondary reference for the ZSM-5 derived materials (103.0 eV) and the silicalites (103.3 eV) (29, 35). Due to the superposition of the V $2p_{3/2}$ signal with the X-ray satellite of the O 1*s* line, the analysis of oxide materials containing low vanadium amounts belongs to the more involved tasks in XPS. Commercial X-ray satellite subtraction routines often leave residual satellite intensity, which interferes with the weak V $2p_{3/2}$ signals. Using an interactive satellite-subtraction routine (36), we were able to adjust the satellite-subtraction parameters to the satellite structure of our X-ray source. In test runs with vanadium-free silicalite samples, this adjustment resulted in a smooth baseline in the V $2p_{3/2}$ region after satellite subtraction, which allowed us to reduce the detection limit for vanadium in vanadium-containing zeolites down to ≈0.2 wt.% (for details cf. (29)), i.e., well below the concentration level for most of the samples used in this study.

V/Si surface atomic ratios given in this paper were calculated from intensity data using the Scofield photoionization cross section data (37) together with an experimentally derived response function of the spectrometer to the variation of the photoelectron kinetic energy.

Electron spin resonance spectroscopy. X-band ESR measurements were performed with the cw spectrometer ESR 300 (Zentrum für Wissenschaftlichen Gerätebau Berlin). The spectra were recorded at room temperature and at 77 K. The magnetic field was measured with reference to the standard 2,2-diphenyl-1-picrylhydrazyl hydrate (DPPH). Simulation of the ESR spectra was done by diagonalization of the spin hamiltonian

$$\mathbf{H} = \beta \cdot \mathbf{S} \cdot \mathbf{g} \cdot \mathbf{B}_0 + D\left(\mathbf{S}_z^2 - S(S+1)\right) + E\left(\mathbf{S}_x^2 - \mathbf{S}_y^2\right) + \mathbf{S} \cdot \mathbf{A} \cdot \mathbf{I}$$

(β is the Bohr magneton, **S** is the total spin operator, **g** is the g-tensor, $\mathbf{B}_0$ is the magnetic field vector, $\mathbf{S}_x$, $\mathbf{S}_y$, $\mathbf{S}_z$ are spin matrices, *D* and *E* are zero field parameters, **A** is the hyperfine tensor, **I** is the nuclear spin operator). For the spectra of isolated VO^{2+} ions ($S = 0.5$), *D* and *E* were taken to be zero while for the spectra of hypothetical V^{4+}–V^{4+} pairs ($S = 1$) various values for *D* and *E* were tried. Relative signal intensities were obtained by double integration of the spectra.

Other methods. IR spectra of adsorbed pyridine were measured in the diffuse reflectance mode with a Perkin–Elmer 1710 Fourier-transform spectrometer. Prior to pyridine adsorption, the samples were pretreated in a flow of nitrogen containing 2% O_2 at 770 K for 1 h. After cooling to room temperature and recording of the zeolite spectrum, pyridine was adsorbed from a nitrogen stream. Prior to acquisition of the spectrum, physisorbed pyridine was desorbed from the pyridine-loaded samples in flowing nitrogen at 423 K for 30 min.

The physical surface area of the vanadium silicalite samples was determined by a simple one-point BET method according to (38). The accuracy of this technique is limited; however, it will be found to be sufficient in the context of the present paper.

The V and Na contents of the zeolites used in this study were determined by ICP-AES after dissolving the samples in a lithium metaborate melt.

RESULTS

Catalytic Properties of Vanadium Zeolites

Figure 1 compares the catalytic activity of vanadyl-exchanged zeolites with that of EL10V1 (1 wt.% V_2O_5/TiO_2). The figure reports X_{NO} (large symbols, full lines) at a space velocity of 94 liters g^{-1} h^{-1} and the trends of Y_{N_2} (small symbols, broken lines), which are given for three examples only to keep the figure comprehensible. The activity data are summarized in Table 1.

NO conversions of ≈95% were found will EL10V1 in a narrow temperature range around 600 K. The N_2 yield, however, fell below X_{NO} under these conditions, which was due to the formation of significant amounts of N_2O. The N_2O amount kept growing with increasing reaction temperature where X_{NO} decreased sharply. At 673 K, the ammonia conversion was almost complete although both NO conversion and N_2 yield were almost equal at ≈0.5. The remaining nitrogen was found as N_2O, which amounted to 20–25% of the feed NH_3. Obviously, NH_3 oxidation to N_2 and/or N_2O took place over EL10V1 to a considerable extent, but it cannot be distinguished whether the N_2O observed was formed

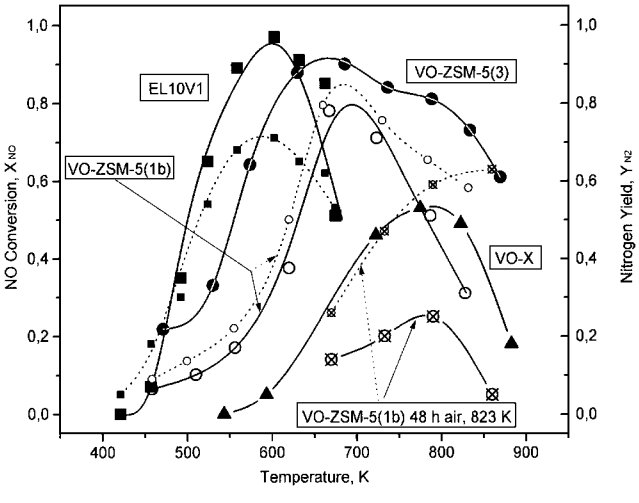

FIG. 1. SCR activity of vanadyl-exchanged zeolites compared with that of V_2O_5/TiO_2. NO conversion (X_{NO}) and N_2 yield (Y_{N_2}) at different reaction temperatures. Feed gas: 1000 ppm NO, 1000 ppm NH_3, and 2% O_2 in He, at 94 liters g^{-1} h^{-1}. Large symbols: NO conversion, left ordinate; small symbols: N_2 yield, right ordinate. N_2 yield omitted for VO–ZSM-5(3) and VO–*X*.

from the reaction of NH_3 with oxygen or with NO. While we found no deactivation of EL10V1 at reaction temperatures $\leq$700 K in the time scale of our runs, a 1-h pretreatment at 823 K in He seriously affected its catalytic behavior: the ammonia conversion decreased to 44% ($T_{max} = 580$ K); at $T \geq 773$ K, negative NO conversions were observed, i.e., NO was formed.

Figure 1 also presents data for two samples prepared by exchange of vanadyl ions into ZSM-5: VO–ZSM-5(3) and VO–ZSM-5(1b). While their V content was almost equal, it will be shown below that the composition of their vanadium phase was different. Both samples were highly active, with peak conversions around 90 and 80%, but there is a difference in the shape of the conversion-temperature curve. It is clear, however, that VO–ZSM-5 may maintain a high activity in a wide temperature region. The nitrogen yield Y_{N_2} (given only for VO–ZSM-5(1b) in Fig. 1) was slightly higher than the NO conversion X_{NO} below the temperature of maximum activity. At higher temperatures, the excess of Y_{N_2} over X_{NO} became somewhat larger. No significant N_2O formation was observed in any run with vanadyl-exchanged zeolites. The increasing excess nitrogen yield indicates therefore an increasing N_2 contribution by ammonia oxidation. A reaction temperature of 873 K caused deactivation also of VO–ZSM-5. Figure 1 shows that already a prolonged calcination (48 h) in air at 823 K proved deleterious for the SCR activity of VO–ZSM-5(1b): After this treatment, the peak conversion fell to 25%, and there was a strong tendency of ammonia oxidation indicated by a high excess of Y_{N_2} over X_{NO}.

In addition, Fig. 1 reports the catalytic behavior of a vanadyl-exchanged Na–X sample. Despite its higher V content (cf. Table 1), the NO conversion achieved with VO–X was much lower than with the VO–ZSM-5 samples, and it attained appreciable levels only at $T \approx 700$ K. This prompted us to focus our further effort on the high-silica MFI zeolites.

Table 1 summarizes the peak NO conversions together with the temperatures at which they were obtained. To provide a better comparison of catalysts with different vanadium content, a normalized reaction rate r(NO)/V at peak conversion was calculated by relating the rate of NO consumption r(NO) to the number of V atoms present. r(NO)/V may be understood as a lower limit of the turnover number, which is not accessible in our case as the percentage of the V atoms engaged in the catalytic reaction is not known. Despite some scatter in the data for different batches of VO–ZSM-5, it is quite obvious that the activity of the V sites in VO–ZSM-5 provides almost the same reaction rate as that of the V in EL10V1 though at a somewhat higher reaction temperature. To avoid conclusions on the basis of reaction rates measured at nearly full conversion, some control experiments were performed at a space velocity of 190 liters g^{-1} h^{-1} (see footnotes to Table 1). They

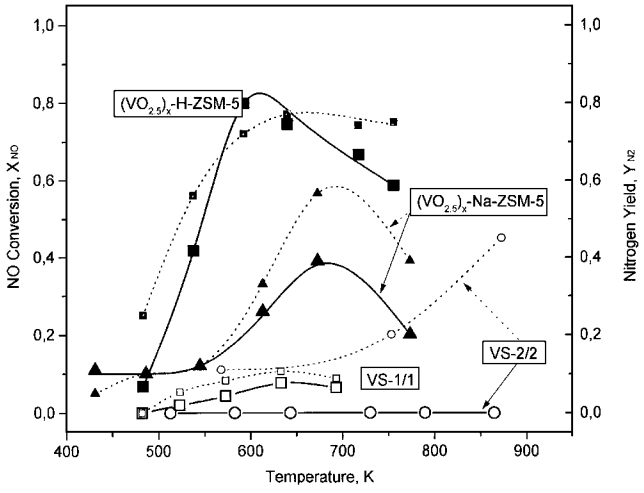

FIG. 2. SCR activity of $(VO_{2.5})_x$–ZSM-5 prepared by CVD of $VOCl_3$, and of vanadium silicalites. NO conversion (X_{NO}) and N_2 yield (Y_{N_2}) at different reaction temperatures. Feed gas: 1000 ppm NO, 1000 ppm NH_3, and 2% O_2 in He, at 94 liters g^{-1} h^{-1}. Large symbols: NO conversion, left ordinate; small symbols: N_2 yield, right ordinate.

confirm that comparable normalized reaction rates may be obtained with V in VO–ZSM-5 and in EL10V1. Severe calcination in air (48 h at 823 K, see lower part of Table 1) decreased r(NO)/V considerably, but it remained still higher than that evaluated for VO–X.

The SCR activities measured with $(VO_{2.5})_x$–ZSM-5 and with the vanadium silicalites are given in Fig. 2 and Table 1. High NO conversions were obtained with CVD-deposited vanadium supported on H–ZSM-5 while the activity of the Na–ZSM-5-derived sample was much lower. This is most likely due to the lower V content of the latter. As a consequence, the normalized reaction rate for V in $(VO_{2.5})_x$–Na–ZSM-5 exceeds that for V in $(VO_{2.5})_x$–H–ZSM-5 significantly. The trends of the N_2 yield were similar to those observed with vanadyl-exchanged ZSM-5, except for a remarkably high contribution of ammonia oxidation with $(VO_{2.5})_x$–Na–ZSM-5. Figure 2 shows further that the SCR activity of the vanadium silicalites is very low. VS-1/1 still brought about some NO conversion whereas the two remaining vanadium silicalite preparations were capable only of ammonia oxidation ($Y_{N_2} = 0.45$ for VS-2/2 at 870 K corresponds to an ammonia conversion of 0.9). To rule out pore blockage as a possible reason for the disappointing SCR activity of these samples, their BET surface area was determined. The results (372, 380, and 271 m^2/g for VS-1/1, VS-1/2, and VS-2/2) prove the accessibility of the internal pore structure in all three cases.

We also tested the SCR activity of our parent ZSM-5 samples. While Na–ZSM-5 was almost inactive, a moderate SCR activity was found with H–ZSM-5, however, at much higher temperatures than with the vanadium-doped samples (Table 1).

Physicochemical Characterization

Figure 3 shows V $2p_{3/2}$ XP spectra of vanadyl-exchanged ZSM-5 samples. The spectral parameters are summarized in Table 2. The spectra of VO–ZSM-5(3) and VO–ZSM-5(1b) in the initial state (upper traces) show how the properties of the vanadium phase were affected by the slight variation of the exchange solution pH (cf. under Experimental). There are two V states with binding energies of 518.4 ± 0.1 and 516.3 ± 0.2 eV (line width (FWHM)—2.4–2.6 eV), which have been assigned to isolated VO^{2+} cations and small intrazeolite $(VO_{2.5})_x$ clusters, respectively (29). From the comparison of V/Si surface and bulk atomic ratios (Table 2) it can be seen that the external surface region of VO–ZSM-5(1b) is strongly enriched in V while those of VO–ZSM-5 samples prepared at pH ≈ 2.8 ((3) and (1a)) are not. This may explain why the signal of the vanadyl cations is hardly discernible in the XP spectrum of VO–ZSM-5(1b) although their presence is demonstrated by ESR (*vide infra*): It is obviously the clustered component that is responsible for the surface enrichment. In VO–ZSM-5(3), and also in VO–ZSM-5(1a), the spectrum of which has been presented in Ref. (29), the V 2*p* signal shape is determined by the high-BE contribution (Fig. 3, Table 2).

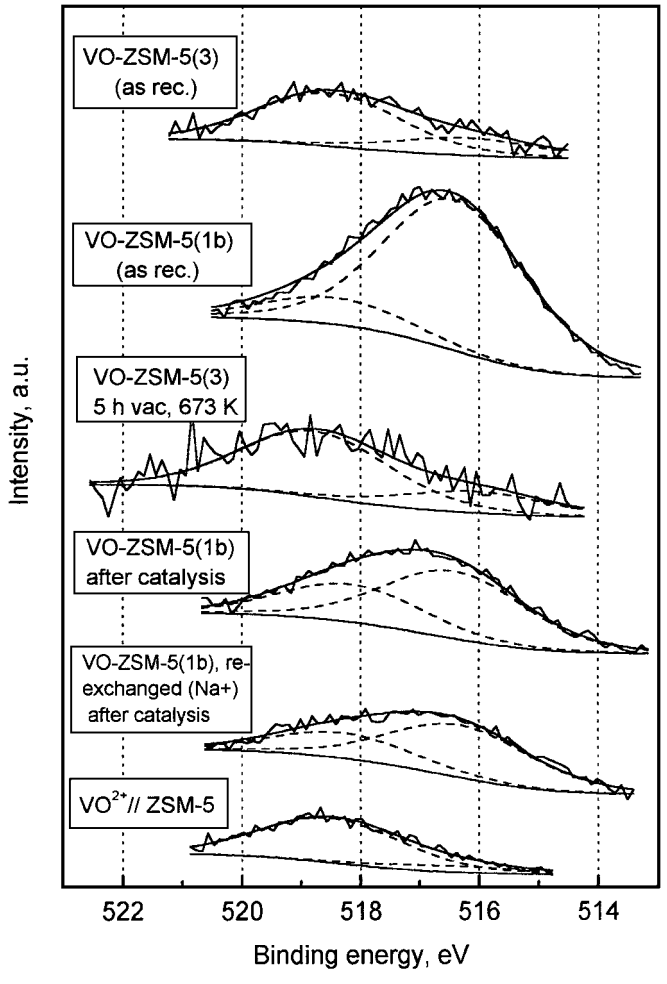

FIG. 3. V $2p_{3/2}$ XPS spectra of vanadyl-exchanged ZSM-5 zeolites after various treatments.

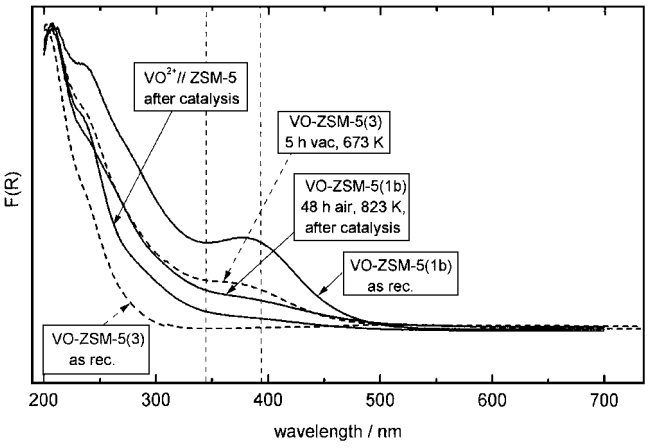

FIG. 4. UV–VIS spectra of vanadyl-exchanged ZSM-5 zeolites after various treatments.

Figure 4 presents UV–VIS spectra of vanadium zeolites investigated in the present study. The differences between the spectra of VO–ZSM-5(3) and VO–ZSM-5(1b) confirm the observations made by XPS. The spectra of samples prepared at pH ≈ 2.8 ((3); the results for (1a) are similar) are dominated by a strong absorption at $\approx$200 nm, which is typical of VO^{2+} cations. At the same time, there is only low intensity in the 350–400 nm region, where a band indicative of V in distorted octahedral coordination as in small intracrystalline VO_x clusters may be expected (21, 28). VO–ZSM-5(1b), however, exhibits large intensity just in this region, which shows that the cluster formation detected by XPS extends into the bulk of the zeolite crystal in VO–ZSM-5(1b) while it is rather a surface phenomenon in VO–ZSM-5(3).

ESR spectra of VO–ZSM-5 samples at 77 and 293 K are reproduced in Fig. 5, where spectrum a refers to the initial material VO–ZSM-5(1b). In addition to a signal with hyperfine structure (hfs) caused by isolated VO^{2+} ions the spectra contain a broad singlet in the range of $g' \approx 2.3$. A similar singlet has also been found in the parent Na–ZSM-5 and arises most probably from Fe^{3+} impurities in oxidic aggregates (39). These are coupled by antiferromagnetic interactions as can be seen by comparing the intensities of the ESR spectra at 77 and 293 K (Fig. 5). For pure paramagnetic behavior the intensity ratio should be $I(77\text{ K})/I(293\text{ K}) = 3.8$ since the magnetic susceptibility is inversely proportional to the temperature according to the Curie–Weiss law. As expected this is valid for the signal of isolated VO^{2+} ions but not for the broad singlet for which lower values are obtained due to the antiferromagnetic interactions.

TABLE 2

Composition of the External Surface Region as Detected by XPS: V/Si Atomic Ratios, Quantitaties of Vanadium Species

Sample	Treatment	$(V/Si)_b$	$(V/Si)_s$	V state	BE (eV)	%
VO–ZSM-5(3)	As received	0.0082	0.0065	VO^{2+}	518.5	75
				$(VO_{2.5})_{x,intra}$	516.1	25
VO–ZSM-5(1a)	As received	0.0044	0.0033	VO^{2+}	518.3	100
VO–ZSM-5(1b)	As received	0.0073	0.027	VO^{2+}	518.5	15
				$(VO_{2.5})_{x,intra}$	516.5	85
VO–ZSM-5(3)	After catalysis	0.0082	0.0061	VO^{2+}	518.3	80
				$(VO_{2.5})_{x,intra}$	516.4	20
VO–ZSM-5(1b)	After catalysis	0.0073	0.013	VO^{2+}	518.2	35
				$(VO_{2.5})_{x,intra}$	516.4	65
VO–ZSM-5(1b)	48 h air, 823 K	0.0073	0.016	VO^{2+}	518.3_5	30
				$(VO_{2.5})_{x,intra}$	516.3	70
VO–ZSM-5(1b)	Na re-exchange after catalysis	0.0040	0.0068	VO^{2+}	518.3	33
				$(VO_{2.5})_{x,intra}$	516.3	67
VO–ZSM-5(1b)	NH_4 re-exchange[a] after catalysis	0.0050	0.0070	VO^{2+}	518.5	90
				$(VO_{2.5})_{x,intra}$	516.4	10
VS-1/1	As received	0.0045	0.0060	V_{iso}[b]	519.1	85
				$(VO_{2.5})_{x,intra}$	516.7	15
VS-1/2	As received	0.014	0.012	V_{iso}	519.0	40
				$(VO_{2.5})_{x,intra}$	516.4	60
VS-2/2	As received	0.021	0.0275	V_{iso}	519.2	15
				$(VO_{2.5})_{x,intra}$	516.6	85
$(VO_{2.5})_x$–H–ZSM-5	As received	0.040	0.18	$(VO_{2.5})_{x,extra}$	517.3	85
				$(VO_{2.5})_{x,intra}$	515.9	15
$(VO_{2.5})_x$–Na–ZSM-5	As received	0.008	0.042	$(VO_{2.5})_{x,extra}$	517.0	100

[a] VO^{2+}//ZSM-5.
[b] Intraframework V.

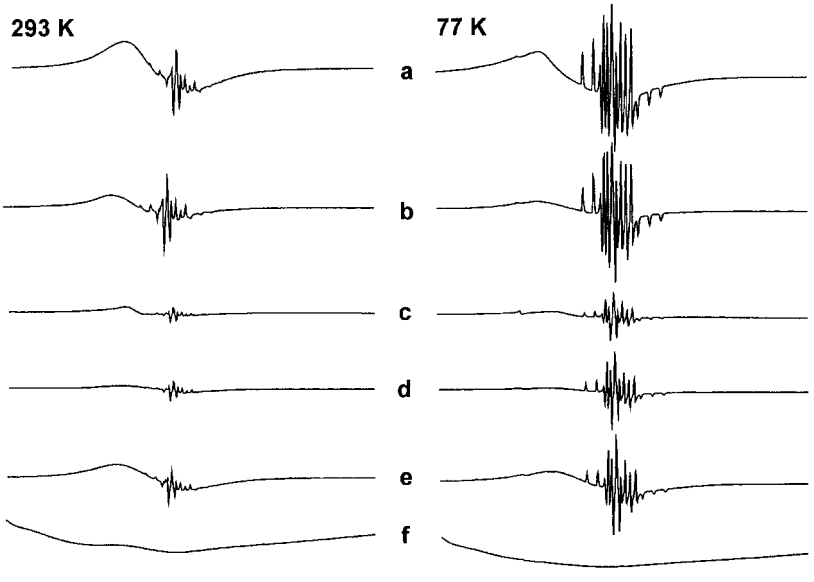

FIG. 5. ESR-spectra of VO–ZSM-5(1b) after different pretreatments measured at 77 and 293 K in the magnetic field range 0–700 mT (identical sample amounts and recording conditions). (a) As received. (b) After catalysis. (c) After 48 h calcination in air at 823 K and catalysis. (d) After re-exchange with $NaNO_3$ and catalysis. (e) After re-exchange with NH_4NO_3 and catalysis (VO^{2+}//ZSM-5). (f) After calcination $+Na^+$ re-exchange and catalysis $(VO_{2.5})_{x,intra}$//ZSM-5).

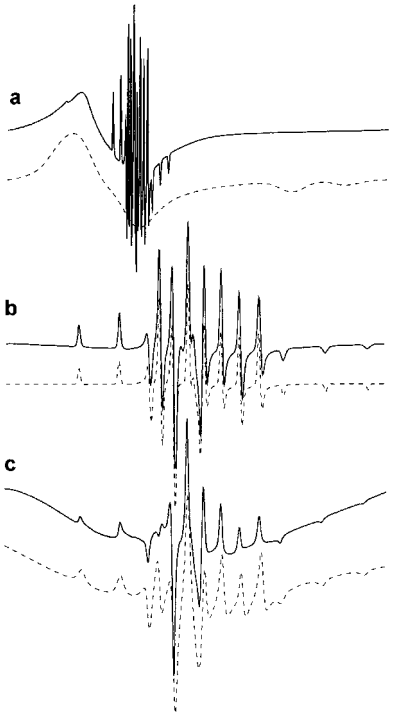

FIG. 6. Experimental (solid line) and calculated (dashed line) ESR spectra. VO–ZSM-5(1b), as-received, at 77 K (a, b) and 293 K, in the magnetic field range 0–1000 mT (a) and 235–435 mT (b, c); calculation parameters: (a) superposition of two spectra with equal intensity: 1. $S = 1$, $g_{\parallel} = 1.93$, $g_{\perp} = 1.98$, $D = 15{,}500$ MHz, $E = 3{,}000$ MHz, line width = 90 mT; 2. $S = 0.5$, $g_{iso} = 2.35$, line width = 150 mT. (b, c) See Table 3.

Notably, we did not find any signal for V(IV) oxide clusters, which should cause a more-or-less broad singlet at $g_{iso} \approx 1.96$. To check whether dimeric V(IV) species ($S = 1$) can contribute to the singlet at $g' \approx 2.3$, a number of spectra with different values for the zero-field splitting parameters D and E were simulated. A signal in this range is predicted for $D = 15{,}500$ MHz and $E = 3{,}000$ MHz (Fig. 6a). However, in this case both allowed transitions cause additional signals in the high-field range ($B_0 > 700$ mT) which were not seen in any of the experimental spectra (Fig. 5). Thus, the presence of even dimeric V(IV) species in our samples is unlikely.

Apart from their intensity, the hfs signals were identical in all samples, indicating that the local structure of the respective vanadyl ions is not influenced by the treatment procedure. The signals can be simulated with the same set of parameters (Fig. 6, Table 3) which are characteristic for immobilized isolated VO^{2+} cations in square-pyramidal geometry (25, 40).

IR spectra of pyridine adsorbed on VO–ZSM-5 samples are presented in Fig. 7. They contain the typical ring modes of pyridine on Lewis sites (1445–1460 cm^{-1}/≈1600 cm^{-1}) or on Na^+ (1445 cm^{-1}/<1600 cm^{-1} (41, 42)), and of pyridinium ions at Brønsted sites (≈1545 cm^{-1}/≈1620 cm^{-1}). The upper traces show the spectra of pyridine on VO–ZSM-5(1b) and VO–ZSM-5(3). From the intense band at ≈1545 cm^{-1} it is quite obvious that the introduction of vanadyl cations into Na–ZSM-5 is accompanied by the appearance of Brønsted acidity.

The structure of the V species is significantly affected by exposure to elevated temperatures as applied in dehydration, calcination, and catalysis. Different changes have been found depending on the temperature range selected in experiments where a cluster-containing sample (VO–ZSM-5(1b)) was treated under severe conditions (oxidizing atmosphere—catalysis or calcination, $T = 823$ K), while an essentially cluster-free material (VO–ZSM-5(3)) was subjected to typical dehydration conditions (5 h evacuation at 673 K). In the XP spectra of these samples (Fig. 3), vanadyl ions and clusters are found to coexist. While the amount of $(VO_{2.5})_x$ clusters has not changed significantly in the surface region of VO–ZSM-5(3) after evacuation at 673 K, it has largely decreased in VO–ZSM-5(1b) after use in catalysis. In addition, the surface of the latter is less enriched in vanadium after the thermal stress at temperatures up to 823 K (cf. Table 2). The UV-VIS spectra (Fig. 4) confirm the trend of cluster *disruption* upon severe calcination as indicated by the lower intensity in the 350–400 nm region of VO–ZSM-5(1b) after 48 h calcination at 823 K. The IR spectrum of this calcined sample after pyridine adsorption

TABLE 3

Spin Hamiltonian Parameters of ESR Signals Detected in Different VO–ZSM-5 Samples (This Work) in Comparison to Those Observed for VO^{2+} in Other Matricees

Signal	$g_{\parallel}$	$g_{\perp}$	$A_{\parallel}$ (mT)	$A_{\perp}$ (mT)	Assignment
hfs, at 77 K	1.9234	1.9716	21.05	7.93	Isolated VO^{2+}
hfs, at 298 K	1.9200	1.9650	20.60	8.30	Square pyramidal
Singlet	$g_{iso} = 2.28$–2.40[a]				Iron oxide clusters, with antiferromagnetic interaction
hfs, at 77 K	1.934	1.988	20.35	8.02	Isolated VO^{2+} in zeolites (25)
hfs[b]	1.924–1.946	1.972–1.987	17.28–20.16	5.43–7.22	Isolated VO^{2+} in V/Al_2O_3 (40)

[a] $I(77\text{ K})/I(298\text{ K}) = 1$–2.
[b] Three signals.

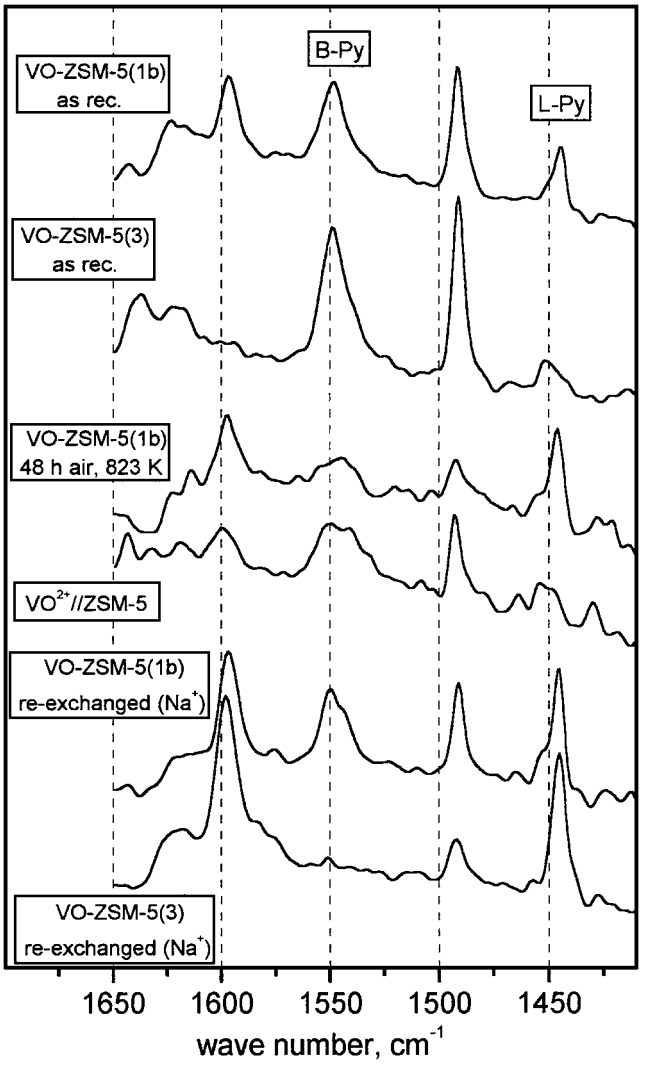

FIG. 7. IR spectra of pyridine adsorbed on VO–ZSM-5 catalysts after various treatments (samples dehydrated in $O_2(2\%)/N_2$ at 773 K for 1 h).

(Fig. 7) shows that the Brønsted acidity has decreased considerably. On the other hand, the UV–VIS spectra taken with VO–ZSM-5(3) (Fig. 4, a similar spectrum was measured with VO–ZSM-5(1a)) indicate that under milder conditions, there is a tendency of cluster *formation*: After evacuation at 673 K (and transfer through air), intensity emerges in the 350–400 nm region, which was quite flat initially. The ESR spectra show that vanadyl ions are lost upon all thermal treatments. After catalysis and calcination, the relative intensities of the hfs signal ((VO^{2+}) ions) decrease considerably (Table 4). After 48 h calcination in air at 823 K, only 10% of the initial amount of VO^{2+} is left.

XP and UV–VIS spectra of the vanadium silicalites and the $(VO_{2.5})_x$–ZSM-5 materials prepared by CVD have been published elsewhere (29). Relevant parameters of the XP spectra are summarized in Table 2. In the spectra of the vanadium silicalites, two V 2*p* signals can be discerned, which have been assigned to isomorphously substituted vanadium (519.1 ± 0.1 eV) and intrazeolite $(VO_{2.5})_x$ clusters (516.5 ± 0.2 eV). The peak fitting results cited in Table 2 show that the VS samples used in this study contain these two types of vanadium species in widely differing proportions. This observation is supported by the UV–VIS spectra of the materials. The absence of surface enrichment and the BE of the $(VO_{2.5})_x$ clusters (< 517 eV, *vide infra*) exclude the presence of significant amounts of extrazeolite vanadium oxide aggregates.

$(VO_{2.5})_x$–ZSM-5 contains vanadium in oxide clusters located on the external zeolite surface as well as in the zeolite pores (29). The V 2*p* XP spectra are dominated by a signal at $\geq$517.0 eV, which is typical of V_2O_5. The external zeolite surface is highly enriched in vanadium (cf. Table 2), and an O 1*s* signal of vanadium oxide ($\approx$530 eV) can be observed together with the zeolite O 1*s* ($\approx$532 eV). The presence of intrazeolite clusters is better proved by UV–VIS spectroscopy, where an intense absorption band in the 350–400 nm region is obvious (29). Additionally, VO^{2+} ions could be observed by ESR in the sample derived from the H-form, but not in that obtained with the Na form (29).

Discrimination of Active Sites

Our results imply that vanadium was present in more than one form in all V–MFI catalysts active in the SCR reaction: VO^{2+} and intrazeolite $(VO_{2.5})_x$ clusters in VO–ZSM-5, extra- and intrazeolite $(VO_{2.5})_x$ clusters in $(VO_{2.5})_x$–ZSM-5. To better understand the catalytic relevance of these V species we attempted to produce samples containing exclusively or predominantly one of them by performing suitable calcination and re-exchange steps with VO–ZSM-5(1b) (see under Experimental): $(VO_{2.5})_{x,\text{intra}}$//ZSM-5 via removal of VO^{2+} by calcination and re-exchange with concentrated NaCl solution, VO^{2+}//ZSM-5 via removal of $(VO_{2.5})_{x,\text{intra}}$ by re-exchange with NH_4NO_3 solution.

TABLE 4

Influence of the Catalyst Pretreatment on the Intensities of the V(IV) hfs Signals

Sample	$I(VO^{2+})_{\text{rel}}$ (at 77 K)	wt.% V
As received	1	0.62
After catalysis	0.6	n.d.
48 h air, 823 K after catalysis	0.1	0.59
Na^+re-exchange, after catalysis	0.3	0.34
NH_4^+ re-exchange (VO^{2+}//ZSM-5), after catalysis	0.3	0.43
Calcination + Na^+ re-exchange ($(VO_{2.5})_{x,\text{intra}}$//ZSM-5), after catalysis	0	0.12

Note. Intensities are related to that in the initial sample, VO–ZSM-5(1b).

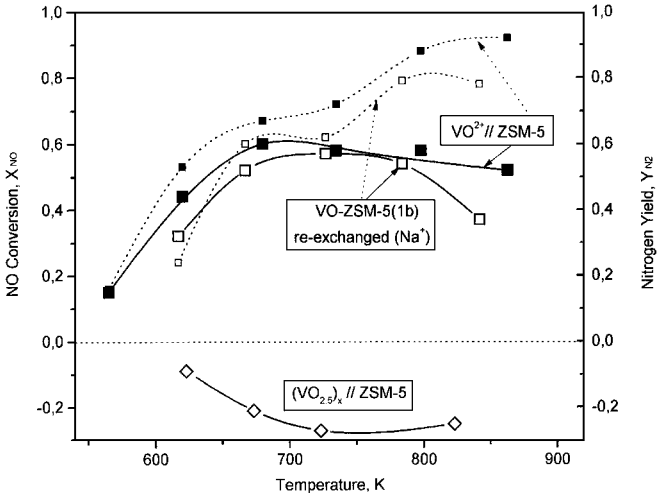

FIG. 8. Catalytic properties of VO–ZSM-5 after various re-exchange procedures. Feed gas: 1000 ppm NO, 1000 ppm NH_3, and 2% O_2 in He, at 94 liters g^{-1} h^{-1}. Large symbols: NO conversion, left ordinate; small symbols: N_2 yield, right ordinate.

Moreover, the influence of Brønsted acidity was examined by re-exchange of VO–ZSM-5 materials with dilute $NaNO_3$ solution.

Figure 8 reports the SCR activities of these samples. Those prepared by treatment with dilute $NaNO_3$ and NH_4NO_3 solutions still exhibited appreciable activities, which was maintained in a wide temperature range in particular after re-exchange with NH_4 ions (VO^{2+}//ZSM-5). In both cases, the N_2 yield was close to the NO conversion up to a reaction temperature of ≈723 K, but ammonia oxidation became more intense at higher temperatures. As re-exchange removes some of the vanadium, the highest normalized reaction rates (Table 1) of the re-exchanged samples even somewhat exceeded that of the initial VO–ZSM-5(1b). Table 1 also reports activity data of a material where the re-exchange with diluted $NaNO_3$ solution had been performed with a sample initially exchanged at pH $\leq$ 2.8 (VO–ZSM-5(1a), not plotted in Fig. 8). Here, a rather low NO conversion was measured, but the degree of vanadium removal was much higher so that the normalized reaction rate of this sample (0.38 min^{-1}) was still of the same order of magnitude found with the other VO–ZSM-5 preparations (0.45–0.62 min^{-1}).

Quite different results were obtained with $(VO_{2.5})_{x,intra}$// ZSM-5, which was prepared by calcination and subsequent Na re-exchange (Fig. 8). X_{NO} was negative over the whole temperature range, which indicates NO formation instead of NO reduction. In addition, N_2O was produced at the lower and higher ends of the temperature range, with a minimum at intermediate temperatures. The opposite trend was found for N_2 formation.

Figure 3 presents XP spectra of VO–ZSM-5(1b) after re-exchange and catalysis (lower traces). Unfortunately, in $(VO_{2.5})_{x,intra}$//ZSM-5, V 2*p* was below the detection limit. After re-exchange with Na^+, the V 2*p* signal shape is not much different from that obtained without re-exchange (VO–ZSM-5(1b) after catalysis). Both vanadyl ions and $(VO_{2.5})_x$ clusters are present in the surface region. Conversely, after re-exchange with NH_4^+ (i.e., VO^{2+}//ZSM-5), the V 2*p* spectrum is dominated by the signal of the VO^{2+} ions, and the signal of the clusters is hardly detectable. This observation is confirmed by the UV–VIS spectrum of the latter sample (Fig. 4): The band in the 350–400 nm region indicative of intrazeolite vanadium oxide clusters is almost absent even after catalysis. In the ESR spectra of the samples prepared by re-exchange with Na^+ and NH_4^+ the hfs signal of isolated VO^{2+} ions is still present although with lower intensity than in the initial VO–ZSM-5(1b) (Fig. 5, spectra d, e, Table 4). In $(VO_{2.5})_{x,intra}$//ZSM-5, however, it could not be detected at all (Fig. 5 spectrum f) indicating that calcination and subsequent Na^+ re-exchange removed isolated VO^{2+} ions completely.

IR spectra of pyridine adsorbed onto VO–ZSM-5 after re-exchange and catalysis are shown in Fig. 7. After re-exchange with NH_4^+ (VO^{2+}//ZSM-5), the most conspicious feature is the strong decline of the bands at 1445 and 1598 cm^{-1} whereas there is, clearly, intensity in the Brønsted region around 1545 cm^{-1}. The spectra obtained after re-exchange with Na^+ contain some surprising features. With VO–ZSM-5(1b), we found a signal of Brønsted sites even after re-exchange with Na^+ while the signals at 1445 and 1598 cm^{-1} became very intense. The latter was observed also upon re-exchange of VO–ZSM-5(3) with Na^+. Here, however, the signal of the Brønsted sites was completey quenched.

DISCUSSION

The results of this study show that it is possible to prepare highly active SCR catalysts by modification of ZSM-5 zeolite with vanadium, in particular by exchange with VO^{2+} cations and by deposition of vanadium oxide clusters. The highest normalized reaction rates are in the same order of magnitude as those measured with the reference V_2O_5/TiO_2 sample and are well comparable with activity data reported in the literature for vanadia–titania catalysts (4, 12), although normalized reaction rates of such systems have been recently improved considerably by application of particular preparation techniques (43). The parent Na–ZSM-5 is essentially inactive, while H–ZSM-5 exhibits some activity at high temperatures. Certainly, the latter does not interfere with the catalytic phenomena dealt with in the present paper because the vanadium-doped samples become active at much lower temperatures. At higher temperatures, their behavior is rather determined by a tendeny to catalyze the competitive ammonia oxidation. The runs with the parent zeolites also exclude a significant influence of the iron

impurity on the results with the vanadium-modified materials.

In the following, we will first present an identification of the V species present in the samples on the basis of our spectroscopical results. We believe that there is a quite reliable basis for the interpretation of our XPS (29), UV–VIS (21, 29), and ESR (25, 40) data. On the other hand, the discussion of our IR spectra will focus on the most obvious aspects, because we feel that an appropriate interpretation of some details will require a more fundamental investigation into the interaction of N bases with vanadium-modified zeolites. Finally, the results of the catalytic and the characterization study will be combined to identify the sites active for the SCR reaction over vanadium-modified ZSM-5 zeolites.

Properties of the Vanadium Phase in V–ZSM-5 Materials

The assignment of V species detected in the vanadium silicalites and in $(VO_{2.5})_x$–ZSM-5 prepared by CVD has been discussed in detail in Ref. (29), and only the key arguments will be outlined here. In the vanadium silicalites, both isomorphously substituted vanadium (V_{iso}, XPS BE >519.0 eV) and intrazeolite V(V) oxide clusters (XPS BE ≈516.5 eV, UV–VIS absorption at 350–400 nm) were detected in widely differing proportions. In VS-1/1, the contribution of $(VO_{2.5})_{x,intra}$ was near the detection level while in VS-2/2, most of the vanadium was present in clustered form. Notably, these clusters were intrazeolite also in the latter sample, which is implied by a V 2*p* BE significantly different from that of V_2O_5, the wavelength of their UV–VIS absorption and by the absence of vanadium enrichment in the external surface region (Table 2).

The $(VO_{2.5})_x$–ZSM-5 materials prepared by CVD of $VOCl_3$ are coated with extrazeolite vanadium oxide aggregates. According to their V 2*p* BE (517.1-2 eV), these might consist of V_2O_5; they did not, however, give rise to any XRD pattern. Their signal dominates the XP spectra and renders the detection of any other vanadium species (e.g., VO^{2+} ions, *vide infra*) extremely difficult because the aggregates largely screen the external layers of the zeolite crystal for a surface-sensitive technique. They are, on the other hand, less visible for the (bulk) UV–VIS spectroscopy (29), which, instead, was able to detect intrazeolite $(VO_{2.5})_x$ clusters by their absorption between 350 and 400 nm. Hence, intra- and extrazeolite vanadium oxide aggregates coexist in the $(VO_{2.5})_x$–ZSM-5 materials, and it may be assumed that the extrazeolite aggregates are larger than the intrazeolite ones. In addition, VO^{2+} ions were observed by ESR in $(VO_{2.5})_x$–H-ZSM-5, but not in $(VO_{2.5})_x$–Na-ZSM-5. It is not established at present how the vanadyl ions are formed in a synthesis route starting from pentavalent vanadium ($VOCl_3$) and including only CVD, hydrolysis, and calcination steps. The vanadium content of the $(VO_{2.5})_x$–ZSM-5 materials is higher when H–ZSM-5 is employed, as the acidic protons are effective anchoring groups for the deposition of $VOCl_3$.

During the exchange of VO^{2+} ions into ZSM-5, some of the vanadium aggregates if the pH exceeds 2.8. The resulting clusters can be detected by XPS (V $2p \approx 516.5$ eV) and UV–VIS (350–400 nm). These spectral characteristics imply a small size and intrazeolite location of the clusters (29) despite their enrichment in the external region of the zeolite crystallites. Notably, the spectral characteristics do not change upon sample calcination. This implies that V is in its highest oxidation state already in the clusters of the as-received samples, which had been subjected to elevated temperatures (383 K) only during drying. Indeed, no clustered V(IV) phase could be detected by ESR in any of the samples studied. VO–ZSM-5 prepared at pH ≤ 2.8 is largely cluster-free. Irrespective of the cluster content, VO–ZSM-5 materials are Brønsted acidic due to the application of an acidic exchange solution (Fig. 7).

Thermal treatment of VO–ZSM-5 induces clustering and oxidation of some of the VO^{2+} ions. The aggregation was revealed by UV–VIS with cluster-free materials, where clusters were detected in VO–ZSM-5(3) after heating at 673 K (Fig. 4). XPS failed to see this trend because the external crystallite regions contained some clustered vanadium already in the as-received state. The loss of VO^{2+} ions at elevated temperatures (catalysis or, in particular, extensive calcination at 823 K) was confirmed by ESR with the cluster-containing material (Table 4). Notably, under the more severe conditions applied to the latter sample, this loss is paralleled not by an increase but by a net loss of V(V) oxide clusters as demonstrated by XPS and UV–VIS (Figs. 3 and 4, spectra of VO–ZSM-5(1b) as received and after catalysis). The decrease of the V/Si ratio in the near-surface region (Table 2) implies that some of the vanadium became mobile under these conditions, because neither the XPS BE nor the UV–VIS wavelength of the corresponding signals indicates a growth of the aggregates. We therefore believe that the clusters were disrupted. The decreased Brønsted acidity of the calcined VO–ZSM-5(1b) (Fig. 7) may indeed suggest that Brønsted sites are consumed in the cluster disruption, although this observation has to be taken with some caution, as the possibility of zeolite dealumination has not been ruled out as yet.

The experimental conditions employed imply that the species resulting from the disruption of V(V) oxide clusters or, possibly, also from a direct oxidation of VO^{2+} ions, are V(V) entities of very low nuclearity, possibly isolated. We speculate that they may be similar to those prepared by Adams *et al.* (13) by esterification of the acidic protons of HNa−Y with $VOCl_3$. In principle, XPS should be able to detect such species, but for an unambiguous assignment, samples containing these structures exclusively will have to be studied. In our recent work (29), we have established well-founded assignments for the V 2*p* BE of

isolated intrazeolite V species: VO^{2+} at 518.4 ± 0.2 eV, isomorphously substituted V(V) at ≥519.0 eV. It is justified to expect a high BE also for extraframework V(V) species of very low nuclearity (or isolated), but there is no basis for any detailed prediction except for the range of 518–519.5 eV. It is therefore quite possible that the signal of the disruption product coincides with that of the VO^{2+} ions. Although the comparison of results from bulk and surface analysis techniques has to be made with greatest caution, the diverging tendencies of the signals assigned to VO^{2+} as observed by XPS and ESR seem to support this interpretation. XPS sees approximately the same vanadyl ion concentration in the external surface region before and after calcination at 823 K (Table 2): By multiplication of the V/Si surface atomic ratio with the percentage of VO^{2+}, we obtain VO^{2+}/Si ratios of 4.0×10^{-3} and 4.8×10^{-3} before and after the heat treatment. In ESR, a tenfold decrease of the vanadyl ion concentration is found.

Upon re-exchange of VO–ZSM-5 with $NaNO_3$ or NH_4NO_3 solutions, some of the V was leached from the zeolite (Table 1). The resulting samples differed significantly in the composition of the vanadium phase. After re-exchange with NH_4^+, both UV–VIS and XPS demonstrate that the zeolite was largely void of clusters even after catalysis (VO^{2+}//ZSM-5 in Figs. 3 and 4). After re-exchange with Na^+, the XP spectrum was similar to that of the starting material after catalysis or calcination (Fig. 3); i.e., the sample probably still contained both clusters and VO^{2+} ions. Notably, there is again a large discrepancy in the (semi) quantitative determination of the vanadyl ion concentrations by ESR and by XPS. Re-exchange and catalysis decreased the ESR signal intensity to ≈30% of the initial value in both samples studied while XPS yielded VO^{2+}/Si ratios of 2.3×10^{-3} and 6.3×10^{-3} with the same samples. Again, it may be suggested that the protons available after re-exchange with NH_4^+ disrupt clusters formed under the conditions of catalysis into more or less isolated V(V) species, the XPS signal of which may coincide with that of the VO^{2+} ions.

The main goal of the IR study included in this investigation was to show that re-exchange of VO-ZSM-5 with $NaNO_3$ solution indeed removes the acidic protons. The outcome was unexpected in several aspects. We propose here a tentative explanation which allows us to draw some conclusions and to mark points of interest for future studies.

Comparison of the two types of VO–ZSM-5 (prepared without or with clusters) after re-exchange with Na^+ revealed a strong contrast in the region typical for Brønsted sites (Fig. 7, lowest traces): This region is flat for the (initially) cluster-free VO–ZSM-5(3), but contains an unexpected intense signal after re-exchange of the cluster-containing VO–ZSM-5(1b). We believe that there is Brønsted acidity associated with the aggregates, which were deposited at a pH of ≈3. Obviously, these sites do not exchange protons with Na^+ offered in a neutral solution as do the zeolite sites. Notably, after the previous discussion of clustering tendencies with VO^{2+} ions, it is likely that the samples subjected to catalysis or simply thermal dehydration should also contain clustered vanadium. Apparently, the properties of such clusters may depend strongly on the conditions under which they have been formed. In summary, even if we could not prove the removal of acidic protons for all samples re-exchanged with Na^+, we still can show that among our re-exchanged samples there are such with very different Brønsted acidity.

The spectra presented in Fig. 7 do not offer a straightforward assignment for bands due to an interaction of the V species present with pyridine. The band at 1445 cm^{-1} in the spectra of Na-containing samples is certainly due to residual or re-exchanged Na^+. Its increase upon calcination of the cluster-containing VO–ZSM-5(1b) may originate from lifting of a blockage by disruption of the blocking clusters. A signal at ≈1452 cm^{-1} is present in all spectra (partly as a shoulder) and may be assigned to isolated V species. For a more detailed discussion of these signals and of some others that appear significant against the somewhat noisy background of our spectra (e.g., at 1464–1466 cm^{-1}, below 1430 cm^{-1}) a more detailed study of the interaction of isolated V species in zeolites with N bases will be required.

Finally, the sample prepared by calcination and re-exchange with concentrated NaCl solution ($(VO_{2.5})_{x,intra}$// ZSM-5) was studied only by ESR due to its low V content. ESR shows that the isolated VO^{2+} ions were indeed completely removed (Fig. 5, spectrum f). The remaining vanadium was present in clustered form or as cluster disruption product. The relation between these forms remains undetermined as their leaching behavior in the NaCl solution is unknown.

Identification of Active Sites

On the basis of the knowledge about the vanadium phase present it is possible to single out the type of V species responsible for the SCR activity observed (Figs. 1, 2, and 8; Table 1).

For the vanadium silicalite materials, it is clear that neither of the V species in them (V_{iso}, intrazeolite V(V) oxide clusters) possesses an appreciable ability to catalyze the selective NO reduction. This is most obvious for the vanadium oxide aggregates, because with those materials containing predominantly clusters (VS-2/2, VS-1/2), the NO conversion was nil in the limits of experimental accuracy whereas there was still a measurable reaction rate with our purest vanadium silicalite VS-1/1. Hence, isomorphously substituted vanadium may be able to catalyze the SCR of NO by NH_3 at a rather low rate.

In VO–ZSM-5, again, clustered and isolated vanadium species are candidates for the active site, which supplies a

very attractive NO reduction rate in this case. Our data provide strong evidence that this site is the VO^{2+} ion. After removing intrazeolite $(VO_{2.5})_x$ clusters from VO–ZSM-5(1b) by re-exchange with NH_4^+, the vanadium exhibited the same activity (normalized reaction rate) as before, which excludes the relevance of the aggregated phase. The activity has to be assigned to VO^{2+} or possibly to the cluster disruption products, which may have coexisted with the latter under the conditions of catalysis (*vide supra*). The same disruption products should be present after prolonged calcination of the initial VO–ZSM-5(1b). The pronounced loss of activity caused just by this calcination suggests their minor relevance for SCR catalysis. The initial sample, which should contain them in lower amounts, was far more active. The concentration of the VO^{2+} ion was found to decrease by calcination (cf. Table 4), as was the ability of the catalyst to reduce NO. Finally, complete removal of VO^{2+} as in $(VO_{2.5})_x$//ZSM-5 completely removed all SCR activity.

The conclusion that intrazeolite V(V) oxide clusters are inactive irrespective of their origin (by-product of isomorphous substitution, hydrolysis of VO^{2+}, thermal clustering/oxidation of VO^{2+}) was quite unexpected; it is, however, well documented by our data. Instead, the NO reduction is catalyzed by a single site, and the results of our re-exchange experiments further imply that this site might be able to function without the cooperation of a Brønsted site. Re-exchange of VO–ZSM-5 with Na^+ though decreased the activity of the V sites, which rendered somewhat lower normalized reaction rates at slightly higher temperatures of peak conversion (Table 1). However, there was still SCR activity at normalized reaction rates in the same order of magnitude as with the original samples although the absence of Brønsted acidity could be proved at least for one of the re-exchanged materials (cf. Fig. 7). While this point certainly deserves further study, our present results suggest that Brønsted acidity may favor the SCR reaction over vanadyl cations; however, it does not seem to be a prerequisite for the function of these sites.

$(VO_{2.5})_x$–ZSM-5 prepared via CVD contains vanadium oxide clusters, which are probably imperfect V_2O_5 crystallites, supported on the external zeolite surface. Although VO^{2+} ions were detected in the material derived from H–ZSM-5, it is obvious that SCR activity may arise also from these extrazeolite aggregates as the Na–ZSM-5-based material, which was void of VO^{2+} ions, was also active. In view of the previous discussion, we believe, however, that the small intrazeolite vanadium oxide aggregates contribute only to unselective reactions.

The identification of a single V site being able to catalyze the SCR of NO by NH_3 is not understood as a challenge to the dual-site mechanisms discussed for bulk V_2O_5 and V_2O_5/TiO_2 catalysts (10). Probably, the intrazeolite aggregates in our sample, though presenting neighboring V atoms, do not provide them in the required functionality (e.g., V=O and V–OH) or cannot keep their bridging oxygen from performing the unselective reaction with NH_3. The small aggregate size may be the reason for the failure. It is, however, quite clear that the SCR of NO with NH_3 is possible at a high rate on a single site. More work will be necessary to elucidate the reaction mechanism supported by this site, the stability of these catalysts toward water and other ingredients of flue gases, and their reactivity toward SO_2.

CONCLUSIONS

The catalytic behavior of vanadium-modified ZSM-5 zeolites in SCR of NO by NH_3 was studied in the temperature range 450–870 K. The catalytic results obtained were combined with the results of physicochemical characterization with various techniques (UV–VIS, XPS, ESR, IR) before and after the catalytic experiments. Different methods of vanadium introduction resulted in materials with widely different behavior in the SCR reaction. V isomorphously substituted into the ZSM-5 lattice was almost inactive. V(V) oxide aggregates deposited into/onto ZSM-5 via CVD and hydrolysis of $VOCl_3$ exhibited appreciable activities. These were, however, exceeded by the activities obtained when vanadyl cations were exchanged into ZSM-5. The latter samples exhibited rates competitive with those provided by a V_2O_5/TiO_2 reference catalyst although at somewhat higher temperatures.

It was shown by UV–VIS, XPS, and ESR that in VO–ZSM-5 subjected to the thermal conditions of catalysis, several vanadium species may coexist: VO^{2+} ions, V(V) oxide aggregates, both of which are directly detectable by at least one of the techniques employed, and V(V) species of very low nuclearity (perhaps isolated). The latter has to be postulated as a product of the disruption of V(V) oxide clusters at elevated temperatures or possibly of direct oxidation of VO^{2+}. From a study of samples in which the amount of these species was purposefully varied by appropriate calcination and re-exchange procedures, VO^{2+}, i.e., a monomeric vanadium site, could be identified as the source of catalytic activity in VO–ZSM-5. The remaining intrazeolite V species produced in this work (intrazeolite V(V) oxide clusters, their disruption products, isomorphously substituted V) are not able to catalyze the selective reduction of NO with an appreciable reaction rate. On the other hand, it was shown that the larger extrazeolite aggregates deposited on the external surface ZSM-5 crystallites via CVD of $VOCl_3$ were active in the SCR reaction.

ACKNOWLEDGMENT

A grant of the Deutsche Forschungsgemeinschaft (DFG), which enabled M.W. to become a member of the graduate college "Dynamic Processes on Solid Surfaces" established at the Ruhr-Universität Bochum, is gratefully acknowledged.

REFERENCES

1. Bosch, H., and Janssen, F. J. J. G., *Catal. Today* **2**, 369 (1988).
2. Käßner, P., Grünert, W., and Papp, H., *Chem. Techn. (Leipzig)* **48**, 77 (1996).
3. Baiker, A., Dollenmeier, P., Glinski, M., and Reller, A., *Appl. Catal.* **35**, 351 (1987).
4. Went, G. T., Leu, L.-J., Rosin, R. R., and Bell, A. T., *J. Catal.* **134**, 492 (1992).
5. Lietti, L., and Forzatti, P., *J. Catal.* **147**, 241 (1994).
6. Inomata, M., Miyamoto, A., Ui, T., Kobayashi, K., and Murakami, Y., *Ind. Eng. Chem. Prod. Res. Dev.* **21**, 424 (1982).
7. Szakacs, S., Altena, G. J., Fransen, T., van Ommen, J. G., and Ross, J. R. H., *Catal. Today* **16**, 237 (1993).
8. Inomata, M., Miyamoto, A., and Murakami, Y., *J. Catal.* **62**, 140 (1980).
9. Janssen, F. J. J. G., van den Kerkhof, F. M. G., Bosch, H., and Ross, J. R. H., *J. Phys. Chem.* **91**, 5921 (1987).
10. Topsøe, N.-Y., Dumesic, J. A., and Topsøe, H., *J. Catal.* **151**, 241 (1995).
11. Topsøe, N.-Y., Topsøe, H., and Dumesic, J. A., *J. Catal.* **151**, 226 (1995).
12. Dumesic, J. A., Topsøe, N.-Y., Slabiak, T., Morsing, P., Clausen, B. S., Törnqvist, E., and Topsøe, H., *Stud. Surf. Sci. Catal.* **75**, 1325 (1992).
13. Adams, R. C., Xu, L., Moller, K., Bein, T., and Delgass, W. N., *Catal. Today* **33**, 263 (1997).
14. Inui, T., Medhhanavym, D., Praserthdam, P., Fukuda, K., Ukawa, T., Sakamoto, A., and Miyamoto, A., *Appl. Catal.* **18**, 311 (1985).
15. Wittington, B. I., and Andersson, J. R., *J. Phys. Chem.* **97**, 1032 (1993).
16. Bhaumik, A., Kumar, R., and Ratnasamy, P., *Sud. Surf. Sci. Catal.* **84**, 183 (1994).
17. Zatorski, L. W., Centi, G., Lopez Nieto, J., Trifiro, F., Belussi, G., and Fattore, V., *Stud. Surf. Sci. Catal.* **49**, 1243 (1989).
18. Miyamoto, A., Iwamoto, Y., Matsuda, H., and Inui, T., *Stud. Surf. Sci. Catal.* **49**, 1233 (1989).
19. Miyamoto, A., Medhhanavym, D., and Inui, T., *Chem. Express* **1**, 559 (1986).
20. Miyamoto, A., Medhhanavym, D., and Inui, T., *in* "Proc., 9th International Congress on Catalysis, Calgary, 1988" (M. J. Phillips and M. Ternan, Eds.), p. 435. The Chemical Institute of Canada, Ottawa, 1988.
21. Centi, G., Perathoner, S., Trifiro, F., Aboukais, A., Aissi, C. F., and Guelton, M., *J. Phys. Chem.* **96**, 2617 (1992).
22. Uguina, M. A., Serrano, D. P., Ovejero, G., Van Griecken, R., and Camacho, M., *Appl. Catal. A* **124**, 391 (1995).
23. Kornatowski, J., Wichterlová, B., Jirkovský, J., Löffler, E., and Pilz, W., *J. Chem. Soc. Faraday Trans.* **92**, 1067 (1996).
24. Martini, G., Francesca Ottaviani, M., and Servalli, G. L., *J. Phys. Chem.* **79**, 1716 (1975).
25. Komorek, I., Romotowski, T., Serwicka, E. M., and Mastikhin, V. M., *Zeolites* **14**, 629 (1994).
26. Klaas, J., Kulawik, K., Schulz-Ekloff, G., and Jaeger, N. I., *Stud. Surf. Sci. Catal.* **84**, 2261 (1992).
27. Klaas, J., Schulz-Ekloff, G., and Jaeger, N. I., *J. Phys. Chem. B* **101**, 1305 (1997).
28. Grubert, G., Wark, M., Grünert, W., Koch, M., and Schulz-Ekloff, G., *Stud. Surf. Sci. Catal.* **105**, 1077 (1997).
29. Wark, M., Koch, M., and Grünert, W., submitted for publication.
30. Wark, M., Brückner, A., Liese, T., and Grünert, W., *Chem. Tech. (Leipzig)* **49**, 97 (1997).
31. Thangaraj, A., Kumar, R., Miraykar, S. P., and Ratnasamy, P., *J. Catal.* **130**, 1 (1991).
32. *Catal. Today* **20** (1994)—Special issue devoted to V_2O_5/TiO_2 Eurocatalysts.
33. Centi, G., *Appl. Catal. A* **147**, 267 (1996).
34. Kortüm, G., "Reflexionsspektroskopie," Springer, Berlin, 1969.
35. Grünert, W., Muhler, M., Schröder, K.-P., Sauer, J., and Schlögl, R., *J. Phys. Chem.* **98**, 10920 (1994).
36. Boyen, H.-G., "MacFit," Surface Analysis Software Package, available at the University of Basle, Switzerland, Institute of Physics.
37. Scofield, J. H., *J. Electron Spectrosc. Relat. Phenom.* **8**, 129 (1976).
38. Haul, R., and Dümbgen, G., *Chem. Ing. Techn.* **35**, 586 (1963).
39. Brückner, A., Lück, R., Wieker, W., Fahlke, B., and Mehner, H., *Zeolites* **12**, 380 (1992).
40. Nowinska, K., and Wieckowski, A. B., *Z. Phys. Chem. N.F.* **162**, 231 (1989).
41. Martin, C., Martin, I., del Moral, C., and Rives, V., *J. Catal.* **146**, 415 (1994).
42. Jiang, M., and Karge, H. G., *J. Chem. Soc., Faraday Trans.* **91**, 1845 (1995).
43. Amiridis, M. D., Wachs, I. E., Deo, G., Jehng, J.-M., and Kim, D. S., *J. Catal.* **161**, 247 (1996).